Trans. Phenom. Nano Micro Scales, 2(1): 78-85, Winter - Spring 2014
DOI: 10.7508/tpnms.2014.01.007

ORIGINAL RESEARCH PAPER

Numerical Study of Operating Pressure Effect on Carbon Nanotube Growth Rate and Length Uniformity

B. Zahed[1], **T. Fanaei S.**[2,*], **A. Behzadmehr**[1], **H. Ateshi**[3]
[1]*Mechanical Engineering Department, University of Sistan and Baluchestan, Zahedan, I.R. Iran*
[2]*Electrical and Electronic Department, University of Sistan and Baluchestan, Zahedan, I.R.Iran*
[3]*Chemical Engineering Department, University of Sistan and Baluchestan, Zahedan, I.R. Iran*

ARTICLE INFO.

Article history
Received 14 May 2013
Accepted 1 December 2013

Keywords
Carbon Nanotube
Chemical Vapor Deposition
Operating Pressure

Abstract

Chemical Vapor Deposition (CVD) is one of the most popular methods for producing Carbon Nanotubes (CNTs). The growth rate of CNTs based on CVD technique is investigated by using a numerical model based on finite volume method. Inlet gas mixture, including xylene as carbon source and mixture of argon and hydrogen as carrier gas enters into a horizontal CVD reactor at atmospheric pressure. In this article the operating pressure variations are studied as the effective parameter on CNT growth rate and length uniformity.

1. Introduction

Carbon nanotube (CNT) was observed in the 1960s and 1970s [1,2], but it didn't attract much attention until it was reported in its discovery article in 1991 by Iijima [3]. After that CNTs, find lots of interests in academic and industrial researches because of its extraordinary mechanical, electrical and thermal properties [4-6]. These superior properties lead to using CNTs in widespread applications. Among these applications are their use as structural materials [7], nanoelectronic devices, field emission devices [8,9], devices for molecular imaging or sensing [10] and so on. These innumerous potential applications made CNTs most popular nanomaterial in recent decades but the bottleneck in the carbon nanotechnology is represented by the growth process. So far, some techniques have been applied to the growth of CNTs, most popular nanomaterial in recent decades but the bottleneck in the carbon nanotechnology is represented by the growth process. So far, some techniques have been applied to the growth of CNTs, among them can be cited to laser ablation of carbon rods [11] and chemical vapor deposition (CVD) [12]. Compared to other methods CVD seems able to satisfy the requirements of a high purity material and a reasonable growth rate then CVD is vastly used [13-15], due to its handling procedure, simplicity and the possibility of high production rate. CNTs growth rate in CVD reactor depends on various parameters such as inlet flow rate, deposition temperature, inlet hydrocarbon concentration and catalyst types [16,17]. These reaction conditions can vary throughout the CVD reactor. Therefore modeling of these systems will provide important aids to study the effects and the contribution of each reaction conditions on the CNTs growth rate with lower cost compared to experimental studies. These studies illustrate the importance of each conditions separately and also could have for understanding the phenomena that happened during the CNTs growth process in the reactor.

[*]Corresponding author
Email address: tahere.fanaei@ece.usb.ac.ir

Nomenclature

C_p	Specific heat of the gas mixture ($J.kg^{-1}.K^{-1}$)
$\mathbb{D}^T$	Multicomponent thermal diffusion coefficient ($kg.m^{-1}.s^{-1}$)
f	Species mole fraction
$\vec{g}$	Gravity vector
H	Molar enthalpy ($J.mole^{-1}$)
I	Unity tensor
$\vec{j}$	Diffusive mass flux vector ($kg.m^{-2}.s^{-1}$)
m_i	Mole mass of the ith species ($kg.mole^{-1}$)
$\vec{n}$	Unity vector normal to the inflow/outflow opening or wall
P	Pressure (pa)
R	Universal gas constant (=8.314 $J.mole.K^{-1}$)
$\mathcal{R}_k$	Forward reaction rate of the kth gas phase reaction ($mole.m^{-3}.s^{-1}$)
$\mathcal{R}_{-k}$	Reverse reaction rate of the kth gas phase reaction ($mole.m^{-3}.s^{-1}$)
$\mathcal{R}_l^s$	Reaction rate for the lth surface reaction ($mole.m^{-2}.s^{-1}$)
t	Time (s)
T	Temperature (K)
$\vec{V}$	Velocity vector ($m.s^{-1}$)
	Greek Symbols
κ	Volume viscosity ($kg.m^{-1}.s^{-1}$)
λ	Thermal conductivity of the gas mixture ($W.m^{-1}.K^{-1}$)
μ	Dynamic viscosity of the gas mixture ($kg.m^{-1}.K^{-1}$)
ν_{ik}	Stoichiometric coefficient for the ith gaseous species in the kth gas phase reaction
ρ	Density ($kg.m^{-3}$)
σ_{il}	Stoichiometric coefficient for the ith gaseous species in the lth surface reaction
τ	Viscous stress tensor ($N.m^{-2}$)
ω	Species mass fraction
	Subscripts
i,j	With respect to the ith/jth species
	Superscripts
c	Due to ordinary diffusion
T	Due to thermal diffusion

Many researches is investigated the effects of various parameters e.g. effects of inlet flow rate, hydrocarbon concentration, reaction temperature and so on. In this regard, Zahed et al. studied effects of inlet flow rate, hydrocarbon concentration and reaction temperature [18,19] Grujicic et al. [20] established a CNT growth model, to explain the details of gas-phase reactions, surface reactions and the included amorphous carbon components in deposited CNTs. Also, Endo et al. [21] proposed a CFD model to predict the deposition rate of nanotubes via catalytic decomposition of xylene in a CVD reactor. Using this model, they calculate the total production rates of CNT with various inlet xylene concentrations. Similar works are done by Kuwana et al. [22], Puretzky et al. [23], Lysaght and Chui [16], and Ma et al. [17] to find the appropriate conditions for CNT film deposition rate using different modeling methods.

In this research, an APCVD technique for production of CNT is modelled, numerically. The inlet gas mixture includes xylene as carbon source and a mixture of argon with 10% hydrogen, as carrier gas. The effects of operating pressure on growth rate and length uniformity has been studied and discussed.

2. Problem formulation

2.1. Physical Model

The studied reactor is a cylindrical hot wall (made of quartz) horizontal reactor with 34 mm diameter, 1.5 m length. The inlet and outlet diameter is 17 mm (Figure 1). Preheater zone is considered from 20 to 50 cm from the inlet section and furnace zone from 60 to 125cm from the inlet.The reactor works at atmospheric pressure. A uniform layer of iron atoms on the furnace wall is considered as a catalyst for surface reactions. Inlet gas mixture, including xylene with certain concentration (3750 ppm) as precursor and argon with 10% hydrogen as a carrier gas continuously enters into the reactor at 300 K. Gas mixture heated up to 513K through the preheater zone and then enters into the furnace zone for which the gas mixture heated up to a certain temperature.

Except for the preheater and furnace walls that are isothermal, other walls considered to be adiabatic.

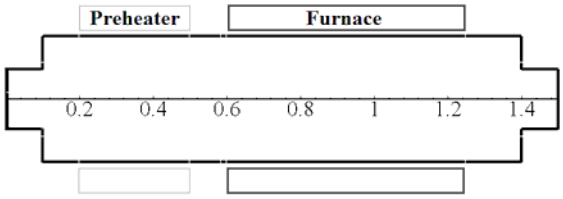

Fig. 1. Geometry of CVD Reactor

Reactor processes is modeled with two gas phase reactions and four surface reactions (Table 1 and 2). These reactions release carbon atoms to growth CNTs on the catalyst particle that layout on the reactor hot walls .

Table 1
Gas phase reactions [21].

Gas Phase Reactions	Pre-Exponential Factor	Activation Energy	TE
$C_8H_{10}+H_2 \rightarrow C_7H_8+CH_4$	2.512e8	1.674e8	0
$C_7H_8+ H_2 \rightarrow C_6H_6+CH_4$	1.259e11	2.224e8	0

Table 2
Surface reactions [21].

Surface Reactions	PEF	AE	TE
$C_8H_{10} \rightarrow 8C + 5H_2$	0.00034	0	0
$C_7H_8 \rightarrow 7C + 4H_2$	0.00034	0	0
$C_6H_6 \rightarrow 6C + 3H_2$	0.00034	0	0
$CH_4 \rightarrow C + 2H_2$	0.008	0	0

PEF=Pre-Exponential Factor, AE=Activation Energy, TE=Temperature Exponent

2.2. Mathematical Model

For modeling the CVD process some assumptions can be used to reduce computational complexity for solving the governing equations. These assumptions are:

- Gas mixture has continuum behavior
- Gas mixture has ideal gas behavior
- Laminar flow regime
- Viscous dissipation is neglected [24]

After assumptions applied to model, governing equations for mentioned model becomes:
Conservation of Mass

$$\frac{\partial \rho}{\partial t} = -\nabla.\left(\rho\vec{V}\right) \tag{1}$$

Conservation of Momentum:

$$\frac{\partial \rho\vec{V}}{\partial t} = -\nabla.\left(\rho\vec{V}\vec{V}\right) + \nabla.\tau - \nabla p + \rho\vec{g} \tag{2}$$

For Newtonian fluids viscous stress tensor is as follows:

$$\tau = \mu\left(\nabla\vec{V} + \left(\nabla\vec{V}\right)^T\right) + \left(\kappa - \frac{2}{3}\mu\right)(\nabla.\vec{V})\mathrm{I} \tag{3}$$

These equations are coupled with energy equation.

Energy Equation:

$$C_p\frac{\partial \rho T}{\partial t} = -C_p\nabla.\left(\rho\vec{V}T\right) + \nabla.(\lambda\nabla T) + \nabla.\left(RT\sum_{i=1}^{N}\frac{\mathbb{D}_i^T}{m_i}\nabla(\ln f_i)\right) + \sum_{i=1}^{N}\frac{H_i}{m_i}\nabla.\vec{J_i} - \sum_{i=1}^{N}\sum_{k=1}^{K}H_i\,\nu_{ik}\left(\mathcal{R}_k^g - \mathcal{R}_{-k}^g\right) \tag{4}$$

and Species Transport Equation:

$$\frac{\partial(\rho\omega_i)}{\partial t} = -\nabla.\left(\rho\vec{V}\omega_i\right) - \nabla.\vec{J_i} + m_i\sum_{k=1}^{K}\nu_{ik}\left(\mathcal{R}_k^g - \mathcal{R}_{-k}^g\right) \tag{5}$$

2.3. Computational fluid dynamics Model

The governing equations are discretized using finite volume approach. For discretize of convection terms in momentum and energy equations, QUICK method, is used. Also central difference method is used for discretizing diffusion terms.

SIMPLE algorithm is adopted for the pressure-velocity coupling. Convergence criterion for energy equation is 10^{-10} and for other equations (continuity, momentum and species transport) is 10^{-6}. After grid test a comparison is performed with Endo et al [21] work to see the accuracy of numerical results. This is

shown in figure 2. As seen good agreement between the results are seen.

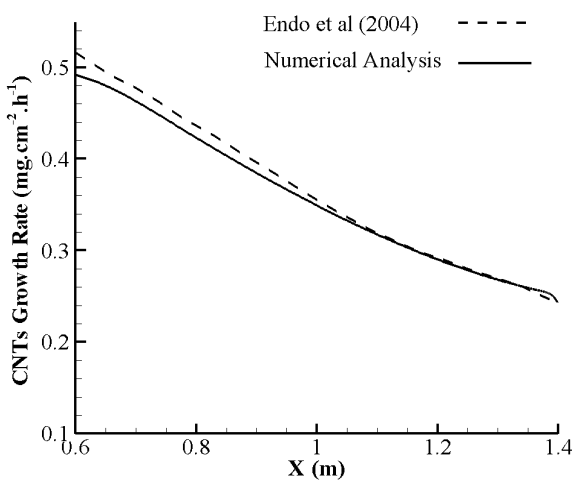

Fig. 2. Validation with Endo et al. work [21]

3. CVD process theory

As known, CNTs growth rate can be calculated using following correlation [25]:

$$SDR = \frac{K_S h_G}{K_S + h_G} \frac{C_T}{N} Y \tag{6}$$

hich:

$$Y = \frac{C_G}{C_T} = \frac{P_G}{P_{Total}} \tag{7}$$

$$P_{Total} = \sum P_{G_i} \tag{8}$$

From (6) seen that surface deposition rate could be controlled by value of h_G and K_S:

- If $K_S \ll h_G$ so:

$$SDR \cong K_S \frac{C_T}{N} Y \tag{9}$$

In this case deposition rate is controlled by surface reaction. Mass transfer through gas boundary layer is fast while the surface reaction is slow.

- If $K_S \gg h_G$ so:

$$SDR \cong h_G \frac{C_T}{N} Y \tag{10}$$

This case is controlled by mass transfer process. In this case surface reaction is quite fast compared to the mass transfer process.

K_S, h_G, Y and C_T represent surface reaction rate, mass transport coefficient, mole fraction of existent species in gas phase and Concentration of all species in gas phase, respectively. So these four parameters have major effect on CNTs total production in CVD reactors.

Moreover mass transfer coefficient depends on diffusion coefficient (D_G) and boundary layer thickness (δ_s) with the following equation:

$$h_G = \frac{D_G}{\delta_s} \tag{11}$$

As known, boundary layer thickness is given by:

$$\delta_s(x) = \left(\frac{\mu x}{\rho U}\right)^{1/2} \tag{12}$$

ρ, μ, U is density, viscosity and velocity of gas mixture. Also x is distance along axis from the reactor entrance.

Also K_s has Arrhenius dependency to temperature as follows:

$$K_S = K_0 \exp\left(-\frac{E_a}{kT}\right) \tag{13}$$

Therefore in chemical vapor deposition there are two distinct temperature regions: controlled by the surface reaction and controlled by the mass transfer. In practice, cross over temperature (where both the surface reaction and the mass transfer through the boundary layer are equal) and the range of temperature corresponding to these regions depends on various parameters such as precursor gases, reaction activation energy, flow conditions in reactor and pressure.

For xylene (as precursor) with studying various temperatures reaction (furnace zone temperature) temperature regions obtained as represented in figure 3 (detailed in later works).

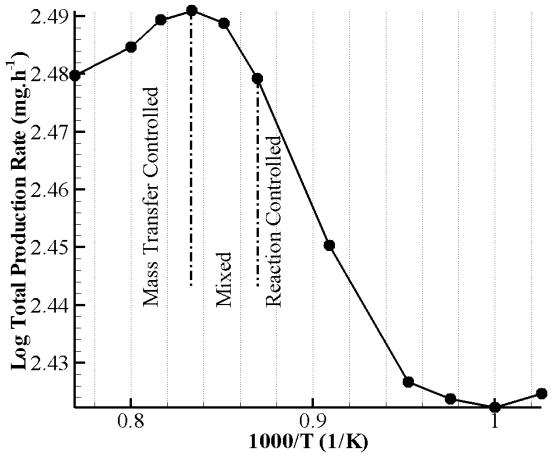

Fig.3. Total production rate versus inverse reaction temperature

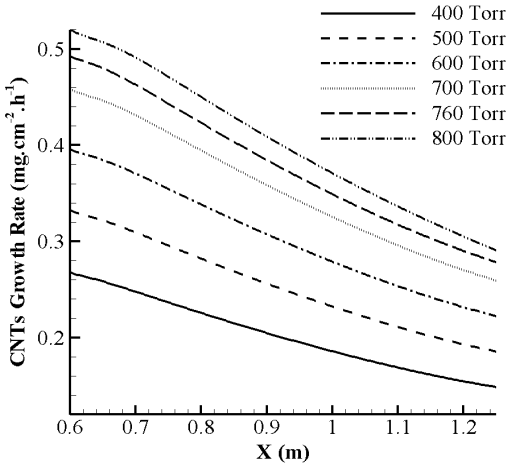

Fig. 4. Local CNTs growth rate with variation of operating pressure in surface reaction controlled region

5. Results and discussion

The effect of operating pressure on carbon deposition rate (that leads to CNTs growth) has been investigated in two distinct thermal regions (mass transfer controlled and surface reaction controlled). Therefore for mass transfer controlled and surface reaction controlled region, furnace temperature is set 1250 K and 975 K, respectively. Operating pressure is considered to be in the range of up to atmospheric pressure**.**

The effects of different pressure on CNTs local growth rate along the furnace region is presented in figure 4 for the reaction controlled region and figure 5 for the mass transfer controlled region. As seen with increasing the operating pressure, growth rate enhances in both thermal zones. To show the effect of operating pressure on total CNT production rate figure 6 is presented.

As seen in both regions, total CNT production rate augment with the operating pressure. Another noticeable result is difference between levels of total production for two regions. As seen total production of mass transfer controlled region is higher than the one for surface reaction controlled region. Because the mass transfer controlled region is operating at the higher temperature region.

To understand such a behavior of CNTs total production versus pressure, in the case of reaction controlled region (reaction temperature is 975K) it could be mentioned that:

Increasing the operating pressure augments the

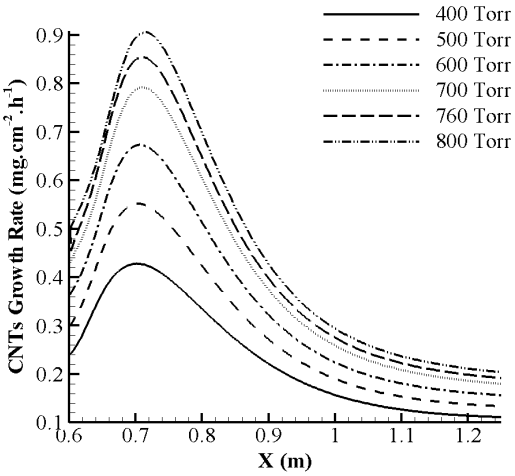

Fig. 5. Local CNTs growth rate with variation of operating pressure in mass transfer controlled region

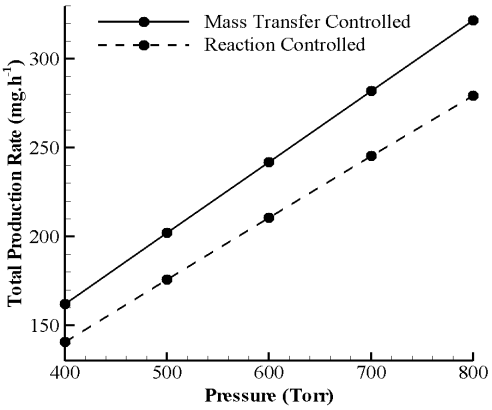

Fig. 6. Total CNTs growth rate with variation of operating pressure in mass transfer and surface reaction controlled region

number of gas species collision. The latter enhances the diffusion coefficient (D_G) across the boundary layer. Thus according to equations 10-12 increasing the operating pressure augments CNTs total production.

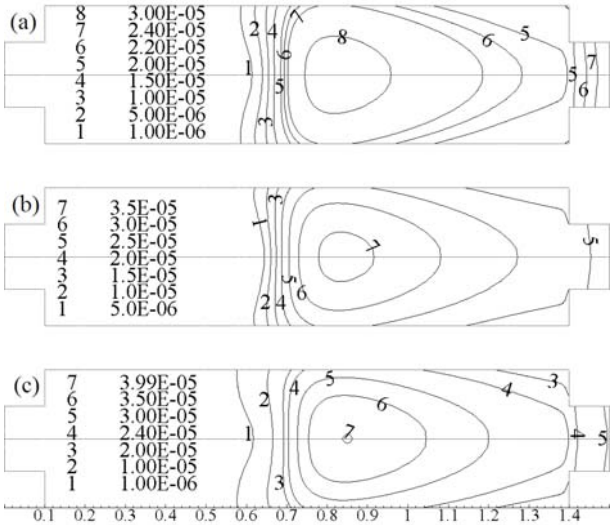

Fig. 7. CH_4 mole fraction throughout the reactor for different operating pressure: (a) 600 Torr (b) 700 Torr (c) 800 Torr in reaction controlled region

Operating pressure has a significant effect on the species mole fractions (Y). As seen in figures 7-9 with increasing the operating pressure from 600 to 800 torr, mole fraction of CH_4, C_6H_6 and C_7H_8 also increase.

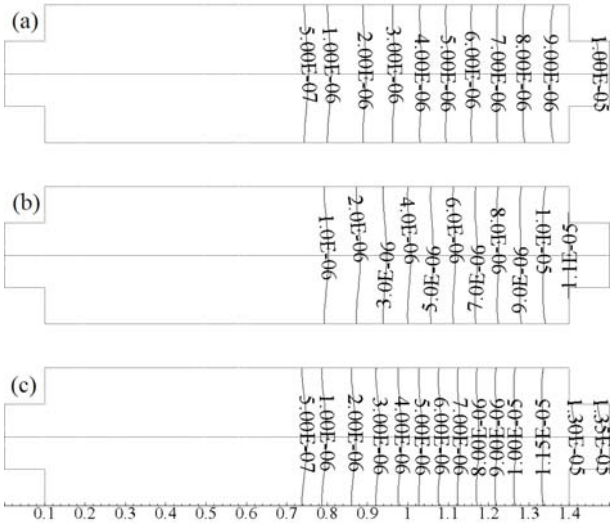

Fig. 8. C_6H_6 mole fraction throughout the reactor for different operating pressure: (a) 600 Torr (b) 700 Torr (c) 800 Torr in reaction controlled region

These increments of the mentioned species mole fractions enhance CNTs total production according to equation 6. However the mole fraction of C_8H_{10} decreases with increasing the operating pressure and consequently causes to decrease CNTs total production.

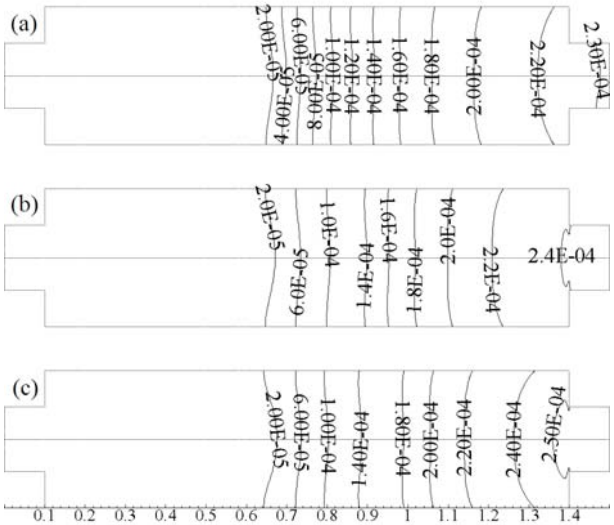

Fig. 9. C_7H_8 mole fraction throughout the reactor for different operating pressure: (a) 600 Torr (b) 700 Torr (c) 800 Torr in reaction controlled region

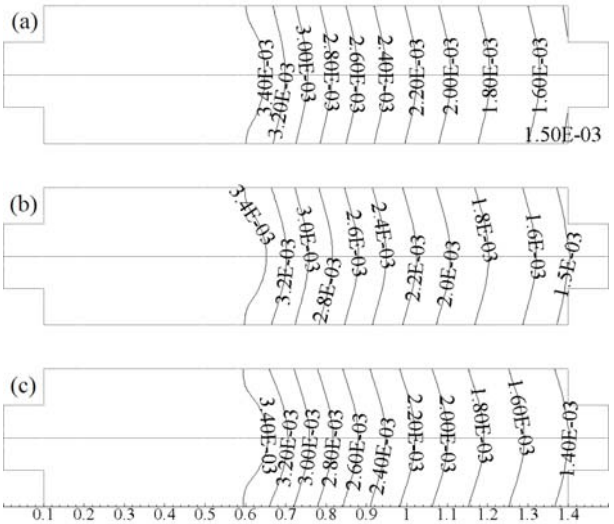

Fig.10. C_8H_{10} mole fraction throughout the reactor for different operating pressure: (a) 600 Torr (b) 700 Torr (c) 800 Torr in reaction controlled region

As seen produced CNTs in mass transfer controlled region has more non uniformity compared to surface reaction controlled region (see figures 4 and 5). To clearly show this characteristic of the produced CNTs the following equation is used:

$$LU = \frac{SDR_{ave}}{SDR_{max} - SDR_{min}} \quad (14)$$

That higher value of LU (length uniformity) shows higher length uniformity of produced CNTs. Figure 11 shows the effect of operating pressure on the uniformity of produced CNTs. As seen the uniformity at the surface reaction controlled region is better than the one at the mass transfer controlled region.

According to equation 11 h_G depends to the boundary layer thickness. Boundary layer thickness varies along the reaction surface and consequently the value of h_G changes. Thus the surface deposition rate is decreased. This leads to significant variation of CNTs production along the reactor and deteriorates length uniformity of the produced CNTs. But in the reaction controlled region that K_s dominates on the surface reaction rate, due to constant reaction temperature, length uniformity of produced CNTs is better.

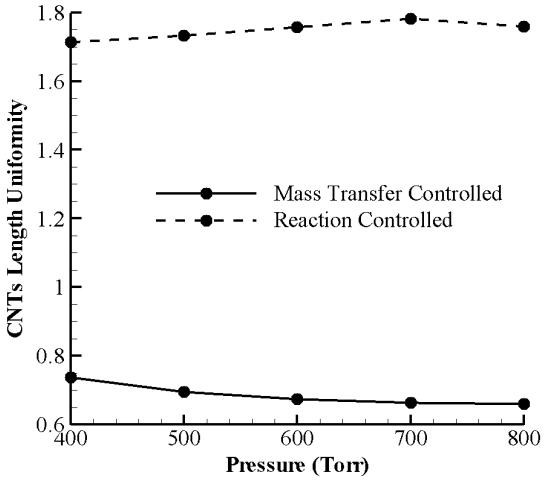

Fig.11. Length uniformity with variation of operating pres mass transfer and surface reaction controlled region

5. Conclusion

The effects of operating pressure on CNTs production rate is investigated numerically. Increasing the operating pressure increases the diffusion coefficient (D_G) and consequently mass transfer coefficient (h_G). Moreover species mole fractions contours shown that increasing of operating pressure augments some of the existent species mole fractions (CH_4, C_6H_6, C_7H_8) that have a positive effect on CNTs total production enhancement.

Also length uniformity of produced CNTs in two temperature regions shows that produced CNTs in surface reaction controlled region has more length uniformity compared to the produced CNTs in the mass transfer controlled region

References

[1] R. Bacon, Growth, Structure, and Properties of Graphite Whiskers, Appl. Phys. Lett. 31(2) (1960) 283-290.

[2] A. Oberlin, M. Endo, T. Koyama, Filamentous growth of carbon through benzene decomposition, J. Crystal Growth 32 (3) (1976) 335-349.

[3] S. Iijima, Helical microtubules of graphitic carbon, Nature 354 (1991) 56-58.

[4] Y.X. Liang, T.H. Wang, A double-walled carbon nanotube field-effect transistor using the inner shell as its gate, Physica E 23 (2004) 232-236.

[5] C. Klinke, A. Afzali, Interaction of solid organic acids with carbon nanotube field effect transistors, Chemical Physics Letters 430 (2006) 75-79.

[6] T.W. Odom, J.L. Huang, P. Kim, C.M. Lieber, Atomic structure and electronic properties of single-walled carbon nanotubes Nature 391(1998) 62–64.

[7] M.M.J. Treacy, T.W. Ebbesen, J.M. Gibson, Exceptionally high Young's modulus observed for individual carbon nanotubes, Nature 381 (1996) 678-680.

[8] S.J. Tans, R.M. Verschueren, C. Dekker, Room-temperature transistor based on a single carbon nanotube, Nature 393 (1998) 49-52.

[9] J.M. Bonard, M. Croci, C. Klinke, R. Kurt, O. Noury, N. Weiss, Carbon nanotube films as electron field emitters, Carbon 40 (2002) 1715-1728.

[10] J. Suehiro, G. Zhou, H. Imakiire, W. Ding, M. Hara, Controlled fabrication of carbon nanotube NO_2 gas sensor using dielectrophoretic impedance measurement, Sensors and Actuators B 108 (2005) 398-403.

[11] A. Thess et al., Crystalline Ropes of Metallic Carbon Nanotubes, Science 273, (1996), 483-487.

[12] R. Andrews, D. Jacques, A. M. Roa, F. Derbyshire, D. Qian, X. Fan, E. C. Dickey and

J. Chen, `Continuous Production of Aligned Nanotubes: a Step Closer to Commercial Realization', Chem. Phys. Lett. 303 (1999) 467-474.

[13] B.C. Liu, S.C. Lyu, S.I. Jung, H.K. Kang, C.-W. Yang, Single-walled carbon nanotubes produced by catalytic chemical vapor deposition of acetylene over Fe-Mo/MgO catalyst, Chemical Physics Letters 383 (2004) 104-108.

[14] Y.S. Cho, G. Seok Choi, G. S. Hong, D. Kim, Carbon nanotube synthesis using a magnetic fluid via thermal chemical vapor deposition , Journal of Crystal Growth, 243 (2002) 224-229.

[15] W. W. Liu, A. Aziz, S.P. Chai, A.R. Mohamed, Tye Ching-Thian, The effect of carbon precursors (methane, benzene and camphor) on the quality of carbon nanotubes synthesized by the chemical vapour decomposition, Physica E 43 (2011) 1535-1542.

[16] A. C. Lysaght, W. K. S. Chiu, Modeling of the carbon nanotube chemical vapor deposition process using methane and acetylene precursor gases Nanotechnology,19(16) (2008) 165607-165614.

[17] L. Pan, Y. Nakayama, H. Ma, Modelling the growth of carbon nanotubes produced by chemical vapor deposition, Carbon 49 (2011) 854-861.

[18] B. Zahed, T. Fanaei S., H. Ateshi, Numerical analysis of inlet gas-mixture flow rate effects on carbon nanotube growth rate, Transport Phenomena in Nano and Micro Scales 1 (2013) 38-45 .

[19] B. Zahed, T. Fanaei S., A.Behzadmehr, H. Atashi, Numerical Study of Furnace Temperature and Inlet Hydrocarbon Concentration Effect on Carbon Nanotube Growth Rate, International J. of Bio-inorganic hybrid nanomaterials 2(1) (2013) 329-336

[20] M. Grujicic, G. Cao, B. Gersten, Reactor length-scale modeling of chemical vapor deposition of carbon nanotubes, J. Mater. Sci. 38(8) (2003) 1819–30.

[21] H. Endo, K. Kuwana, K. Saito, D. Qian, R. Andrews, E.A. Grulke, CFD prediction of carbon nanotube production rate in a CVD reactor, Chem.Phys. Lett. 387 (2004) 307–311.

[22] K. Kuwana, K. Saito, Modeling CVD synthesis of carbon nanotubes: nanoparticle formation from ferrocene, Carbon 43(10) (2005) 2088–95.

[23] A.A. Puretzky, D.B. Geohegan, S. Jesse, I.N. Ivanov, G. Eres, In situ measurements and modeling of carbon nanotube array growth kinetics during chemical vapor deposition, Appl. Phys. A 81(2) (2005) 223–40.

[24] Chris R. Kleijn, C. Werner, Modeling of chemical vapor deposition of tungsten films, Vol 2, *Birkhauser*, Berlin, 1993.

[25] J.D. Plummer, M.D. Deal, P.B. Griffin, Silicon VLSI Technology, Prentice Hall Inc., NewJersy, 2000.